# Regulation of c-Myc and Max in Megakaryocytic and Monocytic-Macrophagic Differentiation of K562 Cells Induced by Protein Kinase C Modifiers: c-Myc Is Down-Regulated but Does Not Inhibit Differentiation[1]

**Ana Lerga, Piero Crespo, Maite Berciano, M. Dolores Delgado, Matilde Cañelles, Carmela Calés, Carlos Richard, Eva Ceballos, Pilar Gutierrez, Nuria Ajenjo, Silvio Gutkind, and Javier León[2]**

Grupo de Biología Molecular del Cáncer, Departamento de Biología Molecular-Unidad Asociada al Centro de Investigaciones Biológicas del CSIC [A. L., P. C., M. D. D., M. C., E. C., P. G., N. A., J. L.] and Departamento de Anatomía y Biología Celular [M. B.], Universidad de Cantabria, and Servicio de Hematología, Hospital Universitario Marqués de Valdecilla [C. R.], Santander, Spain; Departamento de Bioquímica, Universidad Autónoma de Madrid, Spain [C. C.]; and National Institute of Dental Research, NIH, Bethesda, Maryland [S. G.]

## Abstract

**We have studied the regulation and role of c-Myc and Max in the differentiation pathways induced in K562 cells by 12-*O*-tetradecanoyl phorbol-13 acetate (TPA) and staurosporine, an activator and inhibitor, respectively, of protein kinase C (PKC). We found that staurosporine induced megakaryocytic differentiation, as revealed by the cellular ultrastructure, platelet formation, and DNA endoreduplication. In contrast, TPA induced a differentiated phenotype that more closely resembled that of the monocyte-macrophage lineage. c-*myc* expression was down-regulated in K562 differentiated by both TPA and staurosporine, whereas *max* expression did not change in either case. Although PKC enzymatic activity was low in cells terminally differentiated with TPA and staurosporine, inhibition of PKC activity by itself did not induce c-*myc* down-regulation. We conclude that the c-*myc* gene is switched off as a consequence of the differentiation process triggered by these drugs in a manner independent from PKC. Ectopic overexpression of c-Myc in K562 cells did not affect the monocytic-macrophagic and megakaryocytic differentiation, indicating that c-Myc suppression is not required for these processes in K562. Similarly, both differentiation pathways were not affected by Max overexpression or by concomitant overexpression of c-Myc and Max. This result is in contrast with the inhibition of erythroid differentiation of K562 exerted by c-Myc, suggesting divergent roles for c-Myc/Max, depending on the differentiation pathway.**

## Introduction

c-Myc is a nuclear protein of the helix-loop-helix/leucine zipper family that acts as a transcription factor involved in the control of cell proliferation, differentiation, and apoptosis (1–4). c-Myc heterodimerizes through its leucine zipper domain with the protein Max (5, 6). Myc/Max heterodimers transactivate gene expression upon binding to a specific DNA sequence (E box). The interaction with Max is required for all of the biological effects of c-Myc described hitherto. A number of genes have found to be directly regulated by c-Myc, including some involved in cell cycle control, nucleic acid synthesis, and glucose metabolism (7, 8), but most of the complex biological effects exerted by c-Myc are still unexplained. Although expression of *max* is constitutive in most systems, c-*myc* is subjected to extensive regulation during growth and differentiation. The c-*myc* gene is highly expressed in proliferating cells and is down-regulated during cellular terminal differentiation (1, 2).

A model system extensively used to study the role of c-Myc in differentiation is the chemically induced differentiation of human myeloid cell lines. In cell lines such as U937, HL60, HEL, and BM-02, the phorbol ester TPA[3] inhibits growth and induces differentiation into several phenotypes of the myeloid lineage, and in all cases, differentiation is accompanied by c-*myc* down-regulation (9–12). In contrast, no major modification on *max* expression has been found in the cell lines tested (13–15). Because TPA is a PKC activator, the involvement of this family of enzymes in differentiation of hemopoietic cells has received much attention (16). Differential roles for PKC isoforms in myeloid cell differentiation have been reported for human and chicken cells (17–19). TPA-induced differentiation of the human cell lines HL60, HEL, and K562 has been attributed to PKC activation exerted

Received 9/4/98; revised 6/15/99; accepted 7/29/99.
The costs of publication of this article were defrayed in part by the payment of page charges. This article must therefore be hereby marked *advertisement* in accordance with 18 U.S.C. Section 1734 solely to indicate this fact.
[1] Supported by Grant CICYT-SAF96–0083 from the Spanish government and Biomed 96-3532 from the European Community. A. L. and P. G. are recipients of fellowships of the Spanish Ministerio de Educación y Cultura, and M. C. is the recipient of a fellowship from Gobierno Vasco.
[2] To whom requests for reprints should be addressed, at Departamento de Biología Molecular, Facultad de Medicina, 39011 Santander, Spain. Phone: 34-942-201952; Fax: 34-942-201945; E-mail: leonj@medi.unican.es.

[3] The abbreviations used are: TPA, 12-*O*-tetradecanoylphorbol-13 acetate; PKC, protein kinase C; ANAE, α-naphtyl acetate esterase; BrdUrd, bromodeoxyuridine; GFX, bisindolylmaleimide GF109203X; STA, staurosporine; NBT, nitroblue tetrazolium.

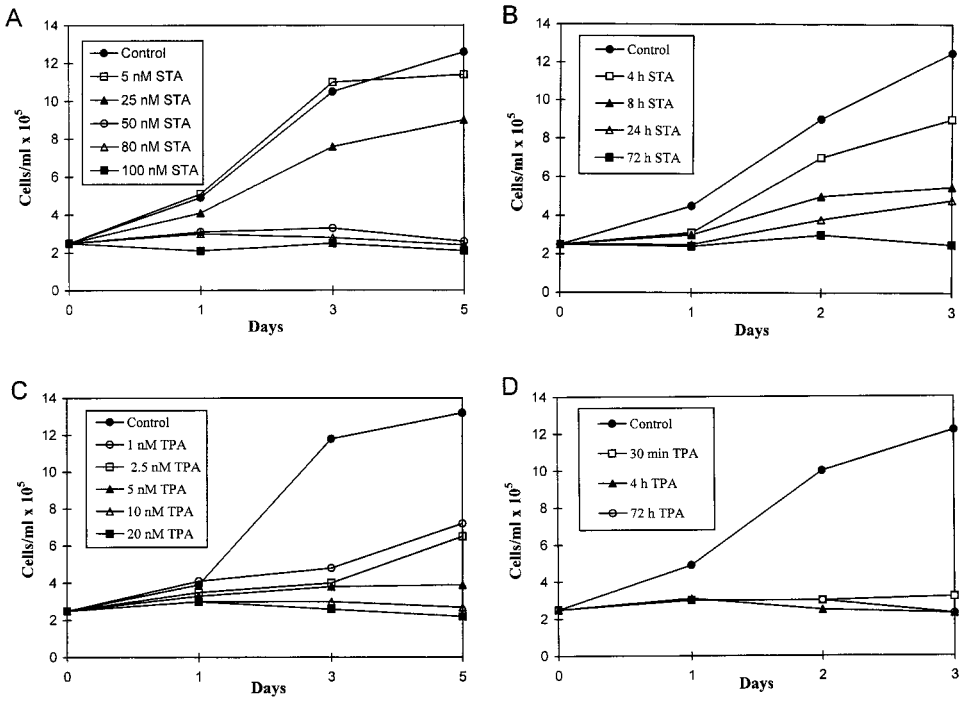


*Fig. 1.* Effect of STA (*A* and *B*) and TPA (*C* and *D*) on cell growth of K562 cells. Growth was determined by counting cell numbers after incubation in the presence of different concentrations of the drugs (*A* and *C*) and after transient exposure to 100 nM STA (*B*) and 10 nM TPA (*D*) for the indicated periods of time. Cell density at the time of drug addition was 250,000 cells/ml. Results are mean values of three independent experiments. SDs were below $1 \times 10^5$ cells/ml for all points.

by this drug (17, 20–22). However, there is confusion about whether c-*myc* down-regulation observed during TPA-induced differentiation is attributable to the activation of PKC, as suggested in some reports (23–25), or rather is a consequence of the cell differentiation process triggered by the drug. In support of the latter idea, spontaneous differentiation of HL60 upon reduction of c-*myc* expression has been described (26–28).

We have investigated the involvement of c-*myc* and *max* in the differentiation of K562 human myeloid cells triggered by modifiers of PKC activity. Because the past studies were hampered by the use of unipotent cell lines, we have addressed this problem by using a multipotent myeloid cell line, which allows the comparison of the role of c-Myc in several differentiation pathways of the same cell line. Human leukemia K562 cells can be differentiated into erythroid cells by 1-$\beta$-D-arabinofuranosylcytosine (29, 30) or into myelomonocytic cells, expressing megakaryocytic, granulocytic, and monocytic markers, by TPA (31–34). We showed previously that ectopic c-*myc* expression impaired erythroid differentiation (15), whereas *max* overexpression increased it (35). We report here that the PKC inhibitor STA induces a clear megakaryocytic phenotype in K562, distinct from that induced by TPA, and we used this model to analyze the regulation and role of c-*myc* and *max* in monocyte-macrophagic and megakaryocyte differentiation pathways. We found that down-regulation of c-*myc* is linked to differentiation but independently of PKC activity. In contrast to their effects on erythroid differentiation, ectopic expression of c-*myc* and *max* does not modify the megakaryocytic and monocytic-macrophagic differentiation pathways.

## Results

**Distinct Differentiation Phenotypes Induced by TPA and STA in K562 Cells.** Treatment of K562 cells with either TPA or STA resulted in cell growth arrest, although with different kinetics. Dose-response assays with STA demonstrated that cell growth arrest and differentiation (described below) were effectively at concentrations >50 nM (Fig. 1*A*). Transient exposure to 100 nM STA for at least 8 h was required to irreversibly arrest and differentiate the cells (see below; Fig. 1*B*). TPA was able to induce growth arrest and differentiation of K562 cells at concentrations of 2.5 nM and above (Fig. 1*C*). Concentrations of 10 nM TPA were chosen for additional experiments. In contrast to the prolonged exposure required for STA-mediated differentiation, treatment with 10 nM TPA for just 30 min induced growth arrest and terminal differentiation (Fig. 1*D*).

TPA treatment committed K562 cells into a well-known phenotype, with loss of the expression of erythroid markers (fraction of cells positive for benzidine reaction and expression of globins) and expression of a series of myeloid-specific markers (33, 36). These include some typical monocyte-macrophage markers such as expression of CD14, phagocytosis, adherence to surfaces and cell cluster formation, positive for ANAE and NBT reduction tests, in addition to markers characteristic of megakaryocytes, such as the expression of glycoproteins IIb-IIIa (CD41-CD61; Table 1). On the other hand, cells treated with STA for 3 days exhibited a phenotype that shared many characteristics with those cells treated with TPA, including the differentiation markers cited above and other less specific markers as vimentin and c-*fos* expression (Table 1). However, significant morphological differences were observed

*Table 1* Differentiation markers in K562 cells treated with TPA and STA

The predominant morphology was determined by May-Grünwald Giemsa staining, and the figures are the mean values from five independent experiments. Marker expression was scored after 3 days of treatment with 10 nM TPA or 100 nM STA. Pluses indicate the percentage of positive cells: −, <10%; +, 10–30%; ++, 30–60%; +++, >60% positive cells. CD61 and CD14 expression were determined by flow cytometry. Cell adhesion was scored by cluster formation. mRNA expression of vimentin, ϵ-globin (after 24 h of treatment), and c-*fos* (after 1 h) was determined by Northern analysis, and pluses indicate their relative expression after film densitometry.

| Predominant cytology | Control | TPA | STA |
|---|---|---|---|
| | Myeloblastic | Monocytic-macrophagic (58 ± 10%) | Megakaryocytic (86 ± 9%) |
| NBT reduction | − | ++ | ++ |
| ANAE reaction | − | ++ | − |
| Cell adhesion | − | ++ | +++ |
| Latex phagocytosis | − | ++ | ++ |
| CD61 | − | +++ | ++ |
| CD14 | + | ++ | ++ |
| Vimentin | + | ++ | +++ |
| c-*fos* | − | +++ | ++ |
| ϵ-Globin | ++ | − | − |
| Glycophorin A | + | − | − |
| Benzidine staining | + | − | − |

between TPA- and STA-treated cells after Giemsa staining, as shown in Fig. 2. Control cells exhibited a homogeneous population of round-shaped cells ~8–10 μm of diameter. The cell nuclei showed a round or oval shape with one or two nucleoli. TPA-treated cells were more heterogeneous. After 3 days of treatment with 10 nM TPA, a majority of cells (58%; Table 1) showed a monocytic-macrophagic morphology, with a higher cytoplasm:nucleus ratio, eccentrically located reniform nuclei, and an irregular cell surface due to projection of lamellipodia (Fig. 2*C*). A smaller fraction of megakaryocytic-like cells were also observed in TPA-treated cells. This fraction accounted for 18% (mean value from five independent experiments) after 3 days of treatment with 10 nM TPA. The rest of the cells retained blastic morphology (Fig. 1*D*). Surprisingly, treatment with STA resulted in the appearance of previously unreported megakaryocyte morphology in most of the cells. These cells were characterized by their large size (~30–50 μm of diameter) and by the presence of a highly lobulated nuclei, giving the appearance of multiple nuclei after Giemsa staining (Fig. 2, *E* and *G*). The fraction of multinucleated cells after STA treatment was close to 100% in some experiments (Table 1). After 5 or more days of treatment with STA, platelet-like bodies could be seen in the cell cytoplasm (Fig. 2*G*) as well as in the extracellular media. Both TPA- and STA-treated cells formed clusters (Fig. 2, *D* and *F*) and adhered to plastic, probably due to the expression of adhesion molecules in the cell surface. However, TPA induced the appearance of fibroblast-like cells (Fig. 2*D*), which were not seen in STA-treated cultures. The cells with megakaryocytic morphology tested negative for the ANAE cytochemical reaction (Fig. 2*I*), which was in contrast with the strong positivity found in TPA-treated cells (Fig. 2*H*). When the STA treatment was prolonged for >3 days, an increasing number of apoptotic cells appeared (19% after 6 days with 100 nM STA; mean from three independent experiments). These apoptotic figures were not seen in TPA-treated cells and are consistent with the recent characterization of the terminal differentiation of megakaryocytes as an apoptotic-like process (37, 38).

To confirm the megakaryocytic phenotype of STA-treated K562 cells, we performed ultrastructural analysis. Untreated cells showed the characteristic morphology of myeloid lineage blasts (Fig. 3*A*). The nucleus contained small compact nucleoli and displayed numerous irregular clumps of condensed chromatin along the nuclear envelope. The perinuclear cytoplasm usually exhibited a centrosomic area with a pair of centrioles, in addition to cisterns of rough endoplasmic reticulum (Fig. 3*B*). The cytoskeletal organization was characterized by the presence of focal accumulations of intermediate filament bundles at the marginal cytoplasm (Fig. 3*C*). After TPA treatment (10 nM; 96 h), the ultrastructural appearance of the majority of the cells was macrophage like. The cell nucleus was eccentrically located, with small aggregates of condensed chromatin associated with the nuclear envelope and nucleolar periphery, as well as extensive domains of dispersed chromatin and large compact nucleoli. The cytoplasm was endowed with phagosomes, lysosomes, lipid droplets, and rough endoplasmic reticulum cisterns (Fig. 3*D*). Also of note was the presence of a prominent network of intermediate filaments running through the cytoplasm, particularly around the nuclei (Fig. 3*E*) and in the cell periphery (Fig. 3*F*). After STA treatment (100 nM; 96 h), most of the cells underwent a dramatic morphological transformation to give megakayocytic cytological features. As such, the cells became large and multinucleated or with highly lobulated nuclei. The nuclei had a predominant pattern of dispersed chromatin with small masses of heterochromatin forming a discontinuous band at the nuclear periphery, in addition to one prominent nucleolus (Fig. 3*G*). The central zone of the cytoplasm showed parallel arrays of channels bounded by endomembranes lacking associated ribosomes (Fig. 3, *H* and *I*). This system of endomembranes clearly resembled the demarcation membranes observed in mature megakaryocytes (39). The intermediate filaments formed a network in the central area of the cytoplasm with prominent fascicles associated with the nuclei (Fig. 3*H*) and running through cytoplasmic areas occupied by demarcation membranes. Some vacuoles, endocytic vesicles, and lysosomes were also observed at the peripheral cytoplasm (Fig. 3*G*).

In view of the prominent presence of intermediate filaments in both TPA- and STA-treated cells (Fig. 3, *E* and *H,* respectively) and the induction of vimentin mRNA expression observed in both types of differentiation pathways (Table 1), we asked whether the filaments observed in the ultrastructural analysis could be formed by vimentin and whether there are differences in the cellular distribution of the filaments between cells differentiated with TPA and STA. Vimentin immunostaining of untreated K562 cells

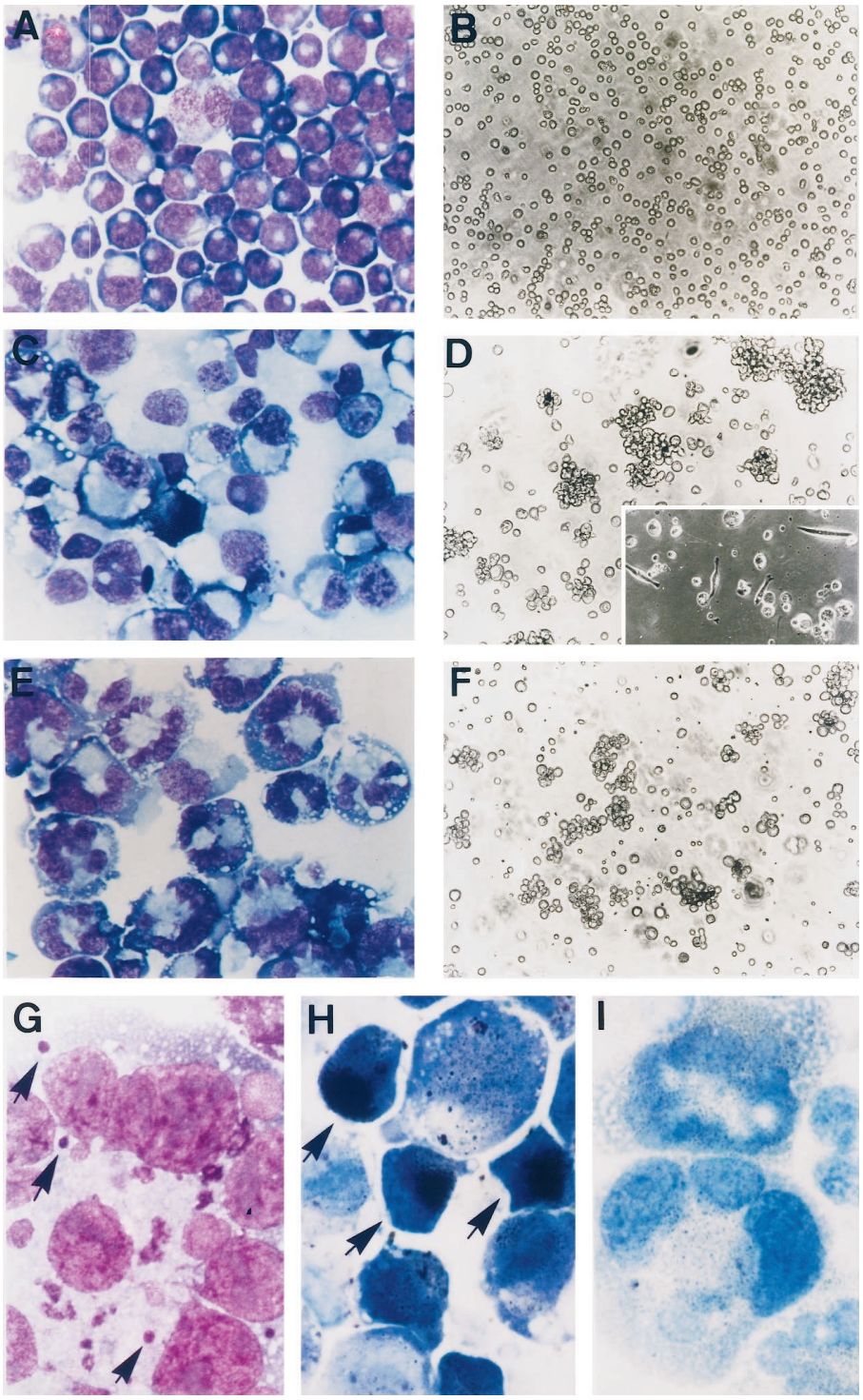


*Fig. 2*. Cell morphology of K562 cells untreated (*A* and *B*) and treated for 3 days with 10 nM TPA (*C, D,* and *H*) or 100 nM STA (*E, F,* and *I*), as indicated. *A, C, E,* and *G*, cytocentrifuge preparations stained by May-Grünwald-Giemsa method (×600). The cells appearing as multinucleated or with polilobulated nuclei are evident after treatment with STA but not with TPA. *G,* a representative cell after 6 days of treatment with 100 nM STA, showing platelet-like forms in the cytoplasm (*arrows*; ×1000). *B, D,* and *F,* phase-contrast micrographs of the cultures showing the clustering induced after 3 days of treatment with 10 nM TPA (*D*) or 100 nM STA (*F*) in standard plastic plates (×200). *Inset* in *D,* fibroblast-like cells appearing after TPA treatment in tissue-culture plates. *H* and *I,* cells subjected to the ANAE test after 3 days of treatment with 10 nM TPA (*H*) or 100 nM STA (*I*). *Arrows,* some positive TPA-treated cells. The negative ANAE reaction is evident in the multinucleated STA-treated cells.

revealed filaments distributed through the cytoplasm that appeared to originate from a polar focus (Fig. 4*A*). In TPA-treated cells, the vimentin pattern displayed a tangle of thick immunostained filament bundles, in addition to thinner fascicles of filaments encircling the cell bodies, just beneath the cell membrane (Fig. 4*B*). Vimentin immunostaining of cells treated with STA for 72 h was characterized by the presence of a marked network of thick filament fascicles concentrated at the central region of the cell and around the nuclei, in contrast with the more dispersed pattern observed in TPA-treated cells (Fig. 4*C*). Overall, vimentin immunostaining of STA-treated cells was more intense than in TPA-treated cells, in agreement with the mRNA expression data (Table 1).

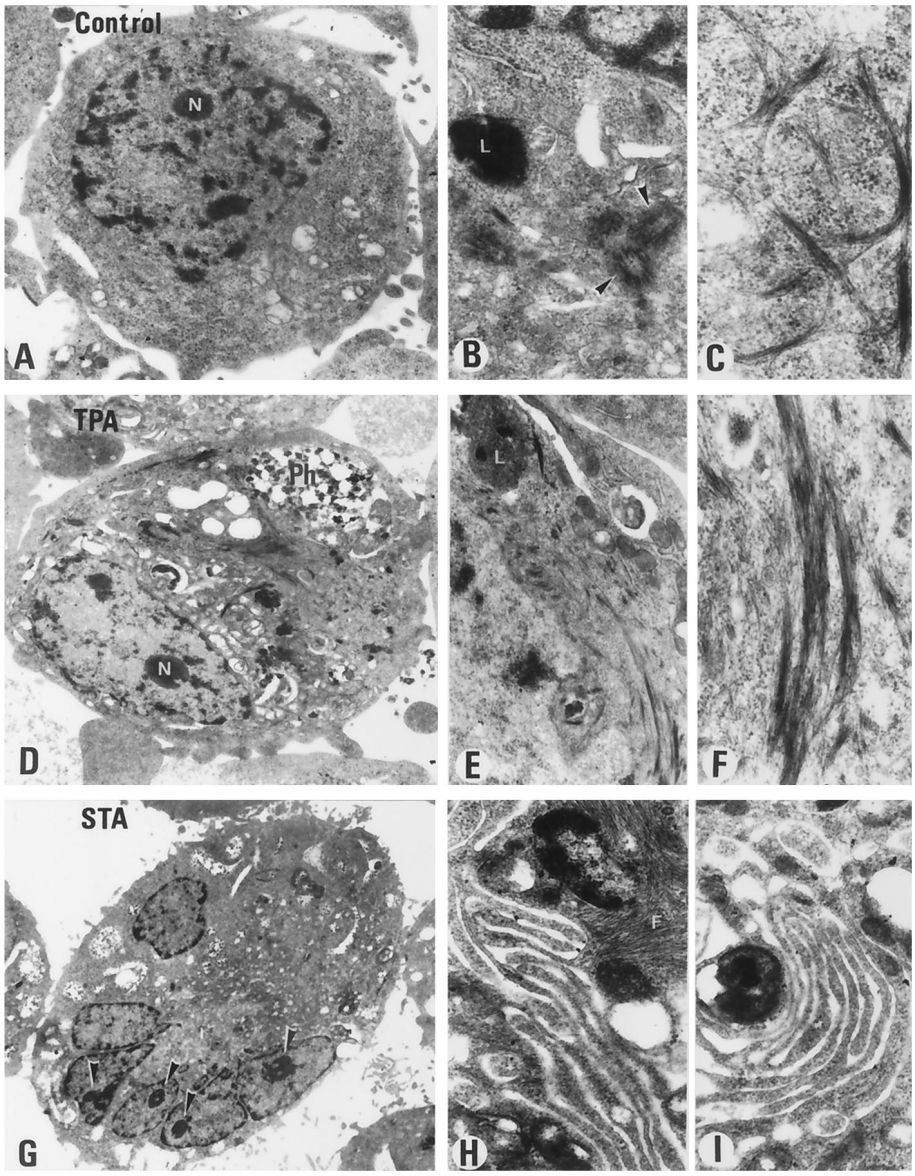


*Fig. 3*. Electron micrographs of K562 control cells (*A–C*), cells treated with 10 nM TPA for 96 h (*D–F*), and cells treated with 100 nM STA for 96 h (*G–I*). *A,* overview of an untreated K562 cell. The cell nucleus shows thread-like masses of condensed chromatin and small nucleoli (*N*). ×8400. *B,* detail illustrating a centrosomatic area adjacent to the cell nucleus, which contains a pair of centrioles (*arrowhead*) and a lysosome (*L*). ×32,000. *C,* detail shows a focal concentration of fascicles of intermediate filaments at the marginal cytoplasm. ×38,000. *D,* overview of a typical TPA-treated cell with a macrophage-like morphology. The nucleus is eccentrically located and presents nucleolus (*N*), small clumps of condensed chromatin at the nuclear periphery, and an extensive central area of dispersed chromatin. The cytoplasm shows phagolysosomes (*Ph*), lipid droplets, and bundles of filaments. ×5500. *E,* detail of the perinuclear region of the cytoplasm containing small bundles of intermediate filaments and a lysosome (*L*). ×12,000. *F,* detail of the peripheral ring of bundles of intermediate filaments. ×38,000. *G,* overview of a typical STA-treated cell. The cell has a large size and shows a megakaryocyte-like morphology. Several small nuclei or nuclear lobules appear displaced at the periphery of the cell body, and in many of them, the nucleoli is apparent (*arrowhead*). Note the presence of clear vacuoles and some endocytic vesicles containing electron-dense particles beneath the cell membrane. ×4250. *H,* detail of the central region of the cytoplasm, which illustrates a lattice of narrow clefts identified as demarcation channels. Note the concentration of intermediate filaments around the nucleus. ×28,000. *I,* detail of cytoplasmic channels bounded by paired demarcation membranes that outlines round or, most frequently, elongated small areas of cytoplasm. ×20,000.

Because the morphological analysis after treatment with STA revealed the presence of multinucleated cells resembling megakaryocytes, we next asked whether these cells were actually polyploid and underwent endoreduplication, a hallmark of megakaryocytic differentiation. The degree of polyploidization in differentiated K562 cells was determined by propidium iodide staining after incubation with TPA or STA for 72 h. DNA analysis showed that the majority (60%) of TPA-treated cells corresponded to cells in $G_0$-$G_1$ phase (2C DNA content), although a significant population (26%) appeared to remain in $G_2$ (Fig. 5*A*). In contrast, more than 50% of STA-treated cells showed a DNA content 4C or higher. In fact, 30% corresponded to cells with 8C DNA content. Thus, K562 cells became polyploid upon treatment with STA but not with TPA. To determine the existence of active S phase, cells differentiated by TPA or STA were incubated with BrdUrd for the final 12 h of the 72-h treatment. As can be seen in Fig. 5*B,* both control and STA-treated cells had incorporated BrdUrd (stained cells over the background level). However, very few BrdUrd-positive cells were detected in TPA-treated cells. Statistical analysis revealed that 25 and 40% of control and STA-treated cells, respectively, showed positive staining. Interestingly, 90% of BrdUrd-labeled control cells corresponded to cells in the $G_1$-S boundary, whereas 95% of the BrdUrd-labeled STA-treated cells corresponded to 4C and 8C DNA-containing cells. Thus, in contrast to TPA-differentiated cells, STA-treated K562 cells undergo active endoreduplication. Altogether these data indicate that STA-induced differentiation resembles that of the megakaryocytic phenotype. Despite the induction of common markers, this differentiation pathway is clearly distinguishable from that induced by TPA, which resembles closer the monocytic-macrophagic.

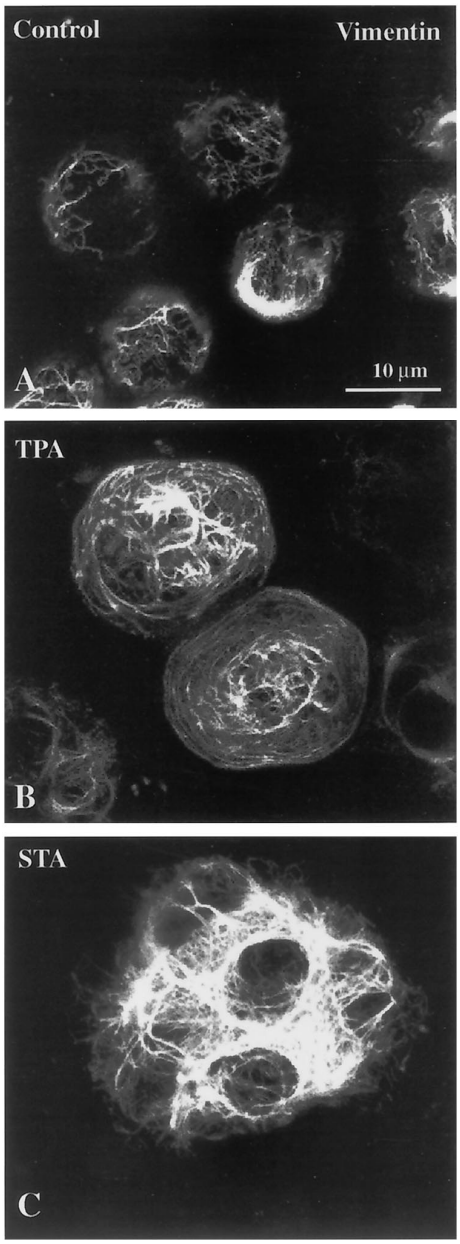


*Fig. 4*. Vimentin immunocytochemistry form control untreated K562 cells (*A*), cells treated with 10 nM TPA for 72 h (*B*), and cells treated with 100 nM STA for 72 h (*C*). Confocal microcoscopy images representing the projection of several Z sections are shown. *Bar,* 10 μm. *A,* untreated cell showing the arrangement of vimentin filaments in a delicate network through the cytoplasm, with a center of vimentin condensation in the cell periphery. *B,* TPA-treated cells showing an eccentrically located tangle of thick vimentin fascicles, in continuity with thinner fascicles that encircle the cell bodies at the marginal cytoplasm. *C,* STA-treated cells showing intense vimentin immunoreactivity in the central region of the cytoplasm. It appears as a network of thick fascicles of filaments, particularly prominent around the nuclei.

**Regulation of c-*myc* and *max* Expression during TPA- and Staurosporine-induced Differentiation.** We have reported previously that c-myc is down-regulated during TPA-induced differentiation of K562 cells (15, 40). We have compared the regulation of c-*myc* and *max* genes during TPA and STA-mediated differentiation. As shown in Fig. 6*A,* the expression of c-*myc* mRNA levels decreased significantly after 12 h of treatment with TPA, at which point the cells were irreversibly differentiated and were almost undetectable after 5 days of treatment. A biphasic regulation of c-*myc* during TPA-mediated differentiation of HL60 cells, with a transient peak after 30–60 min of TPA addition, has been described (24). However, we did not detect such regulation in TPA-treated K562 cells (not shown). c-Myc protein was also dramatically down-regulated in TPA-differentiated cells (Fig. 6*B*). On the other hand, *max* mRNA levels suffered a slight, transient down-regulation after TPA addition, but fully differentiated cells after 3 days of treatment showed no significant changes in mRNA (Fig. 6*A*) and protein levels (Fig. 6*B*).

c-*myc* expression was also down-regulated during treatment with STA at the mRNA and protein levels (Fig. 7). The kinetics of c-*myc* down-regulation during STA treatment is slower than that induced by TPA treatment, as judged by Northern blot (Fig. 7*A*) and by immunoblot (Fig. 7*B*) analysis. c-*myc* mRNA levels dropped by barely 2-fold after 1 day of treatment and reached almost undetectable levels after 5 days. As in the case of TPA, the expression of *max* did not change significantly during STA treatment (Fig. 7). We also tested whether these treatments modify the phosphorylation state of c-Myc and Max. We did not detect major changes on phosphorylation levels of either protein by *in vivo* radiolabeling and immunoprecipitation during TPA and STA treatment (not shown).

**Inhibition of PKC Activity Does Not Induce Differentiation of K562 Cells and Does Not Modify c-*myc* and *max* Expression.** Although TPA is reported to be an activator of PKC activity, STA inhibits PKC as well as other kinases (41, 42). The finding that c-*myc* was down-regulated during differentiation induced both by TPA and STA suggested that the observed c-*myc* suppression was associated with differentiation rather than with PKC activity. To test this possibility, we measured PKC enzymatic activities during TPA- and STA-mediated differentiation. In agreement with the described effect of both drugs, PKC activity was suppressed by STA and was activated by TPA addition, with maximum activity after 5 min (Fig. 8*A*). This result is consistent with the PKC translocation detected shortly after TPA addition described previously in K562 cells (43). We also determined PKC activity in cells irreversibly differentiated by both drugs, *i.e.,* 24 h after drug addition. Interestingly, in K562 cells treated with 10 nM TPA for 24 h, PKC activity was found to be only 15% of that detected in untreated cells (Fig. 8*B*) and similar to that observed in cells treated with high TPA concentrations (1 μM), at which PKC-α, PKC-β, and PKC-ε isoforms, known to be expressed in K562 cells (43), are down-regulated (41). Similar low PKC activities were found after 72 h of treatment (not shown). Thus, treatment with either TPA or STA resulted in repressed PKC activity in differentiated cells, despite the initial PKC activation exerted by TPA.

The former result raised the possibility that c-*myc* down-regulation and cellular differentiation were two processes independently linked to the suppression of PKC activity. To

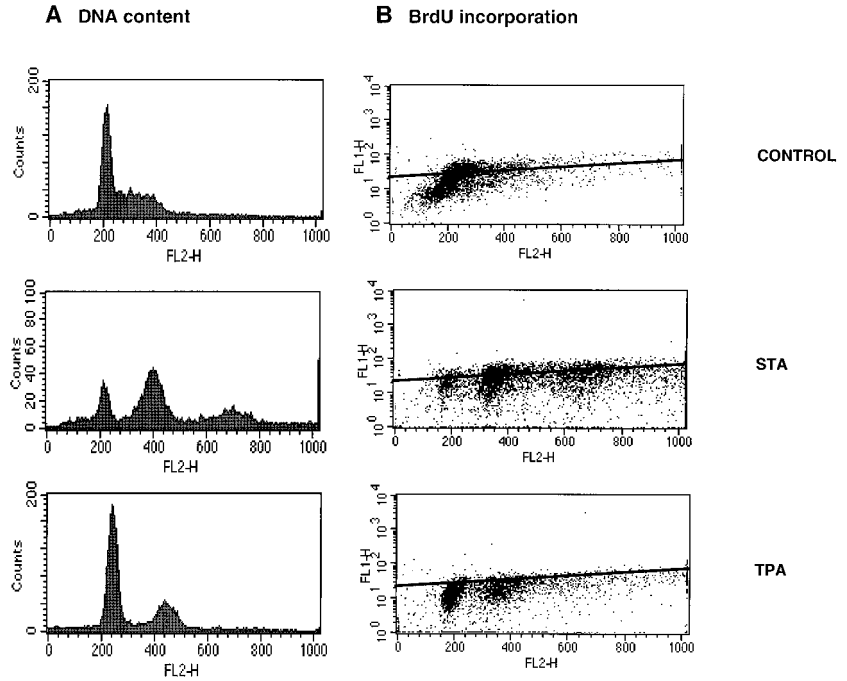


*Fig. 5.* Flow cytometric analysis of DNA content and BrdUrd incorporation. K562 cells were cultured in the absence of drugs (*CONTROL*) or in the presence of 100 nM STA or 10 nM TPA for 72 h. Cell densities at the time of drug addition were 250,000 cells/ml and reached about $1.2 \times 10^6$ cells/ml in the untreated culture. DNA content and BrdUrd incorporation were determined as described in "Materials and Methods." *A,* propidium iodide staining. *Vertical axis,* relative number of cells. *Horizontal axis,* relative DNA content/cell. *Leftmost peak,* cells with 2C DNA content, corresponding to $G_1$ phase. *Middle peak,* cells with 4C DNA content, corresponding to $G_2$-M phase of diploid cells (control cells) and to $G_1$-S phase of tetraploid cells. *Rightmost peak,* cells with 8C DNA content, corresponding to octaploid cells. Cells in S phase appear between 2C and 4C peaks. *B,* BrdUrd immunofluorescence and propidium iodide staining. *Vertical axis,* relative BrdUrd labeling per cell. *Horizontal axis,* relative DNA content/cell. *Bar,* limit of background fluorescence, corresponding to cells cultured in the absence of BrdUrd and incubated with both primary and secondary antibodies.

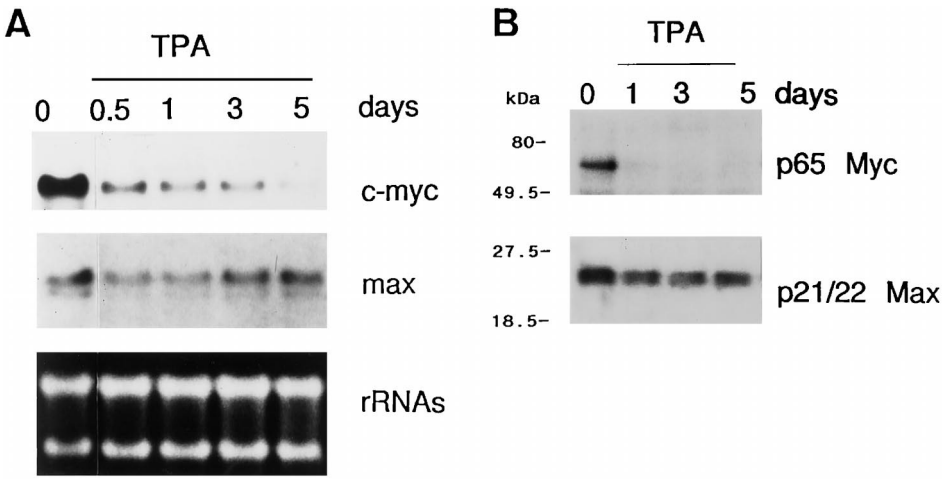


*Fig. 6.* c-*myc* and *max* expression in K562 cells treated with TPA. *A,* expression of c-*myc* and *max* in K562 cells during TPA treatment was analyzed by Northern blot as described in "Materials and Methods." Cells were treated with 10 nM TPA for the indicated periods of time. *Lane 0,* control cells prior to drug addition. The filter was consecutively hybridized to the indicated probes. A picture of the filter after transfer is shown to assess the loading and integrity of the RNAs. *B,* expression of c-Myc and Max proteins in K562 cells during TPA treatment was analyzed by immunoblot as described in "Materials and Methods." Cells were treated with 10 nM TPA for the indicated periods of time. *Left,* position of molecular mass markers.

explore this possibility, we first asked whether PKC downregulation was sufficient for the differentiation of K562. We approached this question by using GFX, a more specific inhibitor of PKC than STA (44). Treatment with 2 $\mu$M GFX resulted in a 75% inhibition of PKC activity (Fig. 8*B*). However, GFX did not cause cell growth arrest nor induced any sign of monocytic or megakaryocytic differentiation, and GFX-treated cultures reached similar cell densities as untreated cells, around $12 \times 10^5$ cells/ml. We next analyzed the effect of GFX on TPA-mediated differentiation of K562. Pretreatment for 1 h with GFX abolished the differentiation induced by TPA, as shown by the absence of cell growth arrest and inhibition of cluster formation (Fig. 9*A*). As expected, preincubation with GFX for 1 h blocked TPA-induced PKC activation (Fig. 8*B*). On the other hand, STA-induced differentiation was not inhibited by GFX or TPA pretreatments (Fig. 9*A*). When STA was added prior to TPA treatment, the differentiation phenotype observed was that of STA alone, with >80% of cells with megakaryocytic morphology after 3 days of treatment (not shown).

Expression of c-*fos* is reported to be induced by TPA in most cells types, including K562 (45), and is considered a molecular marker of PKC activity. Therefore, we analyzed c-*fos* induction in K562 after treatment with TPA and STA. Both drugs induce c-*fos* (Table 1), although with different kinetics; its expression peaked 6 h after TPA addition and 1 h after STA addition (not shown). As shown in Fig. 9*B,* preincubation with GFX 1 h before TPA addition blocked the dramatic induction of c-*fos* expression elicited by TPA. However, GFX did not block c-*fos* induction mediated by

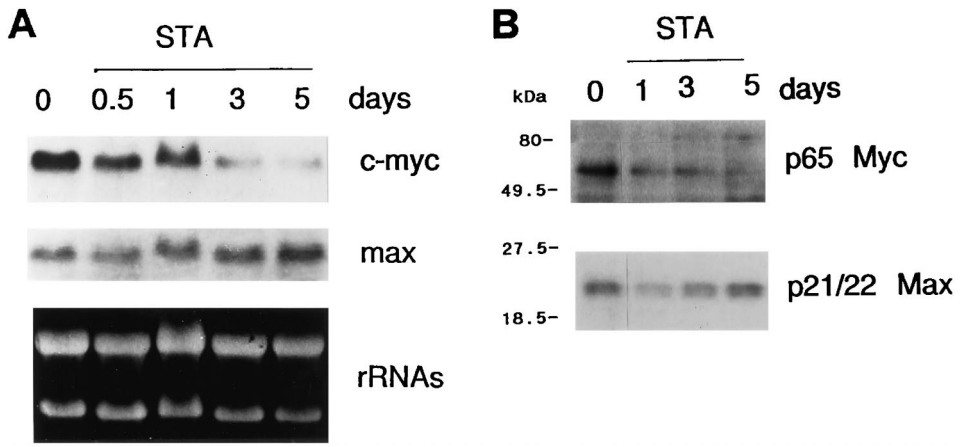


*Fig. 7.* c-*myc* and *max* expression in K562 cells treated with STA. *A,* expression of c-*myc* and *max* mRNA in K562 cells during TPA treatment was analyzed by Northern blot as described in "Materials and Methods." Cells were treated with 100 nM STA for the indicated periods of time. *Lane 0,* control cells prior to drug addition. The same filter was consecutively hybridized to the indicated probes. A picture of the filter after transfer is shown to assess the loading and integrity of the RNAs. *B,* immunoblot of c-Myc and Max proteins in K562 cells treated with 100 nM STA for the indicated periods of time, and the blots were incubated with anti-Myc and anti-Max antibodies. *Left,* position of molecular mass markers.

STA (Fig. 9*B*). Altogether, these results indicate that PKC inhibition *per se* does not induce differentiation of K562 cells but are consistent with the hypothesis that TPA-induced differentiation is mediated by PKC. Thus, the observed down-regulation of PKC activity in TPA-treated cells appears to be a late event in monocytic-macrophagic differentiation of K562.

The expression of c-*myc* and *max* was studied in K562 cells treated with 2 $\mu$M GFX for up to 48 h. Northern blot analysis revealed that the steady-state mRNA levels for both genes did not vary significantly after 24 and 48 h of treatment (Fig. 10*A*), when PKC activity decreased to about 35% of control levels (Fig. 8*B*). A slight decrease in c-*myc* expression was observed after 2 days, but a similar drop was also found in nontreated cells. Thus, this decrease can be associated to growth arrest occurring at high cell densities. Immunoblot with anti-Myc and anti-Max antibodies confirmed that GFX did not significantly decrease c-Myc and Max protein levels (Fig. 10*B*). Therefore, we conclude that the inhibition of PKC activity by itself does not modify c-*myc* expression in K562 cells.

**Enforced c-Myc Expression Does Not Interfere with Differentiation Induced by TPA or STA.** In view of the observed c-*myc* down-regulation after TPA and STA treatments, we tested whether ectopic c-*myc* overexpression had an effect on the differentiation elicited by both drugs. To avoid differences due to individual behaviors of the selected clones, we carried out this analysis on cells transfected with an inducible c-*myc* gene. We used the KmycJ cell line, a derivative of K562 expressing a zinc-inducible c-*myc* (15). Induction of c-*myc* by addition of $ZnSO_4$ resulted in a marked expression of c-*myc*, detected at the mRNA (Fig. 11*A*) and protein levels (Fig. 11*B*). The smaller mRNA detected in the Northern blots reveals the expression of the exogenous c-*myc* gene, because the transfected construct lacks the first untranslated exon (46). As described previously (14, 46), enforced expression of c-*myc* down-regulated the endogenous c-*myc* mRNA (Fig. 11*A*). This well-described effect occurs at the transcriptional level (47), suggesting that the ectopically expressed c-Myc is entering the nuclei of K562. To directly test this, we performed immunocytochemistry with anti-c-Myc antibody and found that c-Myc was present in the nuclei of STA- and TPA-treated cells in the presence of zinc but could not be detected when the cells were differentiated in the absence of zinc (Fig. 11*C*).

We then analyzed whether c-*myc* overexpression impaired TPA-mediated differentiation. Cells were pretreated with 75 $\mu$M $ZnSO_4$ for 2 h to assure that c-*myc* expression was elevated at the time of TPA addition and its expression levels maintained during the treatment. c-Myc overexpression did not modify the differentiation induced by 10 nM TPA, as assessed by vimentin and CD61 expression, NBT reduction assay (not shown), and cell morphology and adherence (Fig. 11*D*), confirming previous results (15). Similarly, c-Myc overexpression did not impair differentiation induced by 2 nM TPA (not shown), the minimal differentiation-inducing concentration (Fig. 1*C*). We next studied whether c-*myc* overexpression modified the megakaryocytic differentiation induced by STA (100 nM). As confirmed by Northern (Fig. 11*A*) and immunoblot analysis (Fig. 11*B*), exogenous c-*myc* expression was clearly induced by zinc. In the presence of STA, despite the elevated levels of c-Myc, the cells showed a differentiated phenotype almost identical to cells differentiated with STA in the absence of zinc. This was assessed by cell morphology, cluster formation (Fig. 11*D*), and expression of markers as NBT reduction and vimentin and CD61 expression (not shown). Likewise, enforced expression of c-Myc did not modify the differentiation induced by 50 nM STA, the lowest concentration that brought about differentiation. Similar results were obtained with KmycB, another c-*myc*-transfected K562 subline (not shown). From these experiments, we conclude that c-Myc down-regulation is a

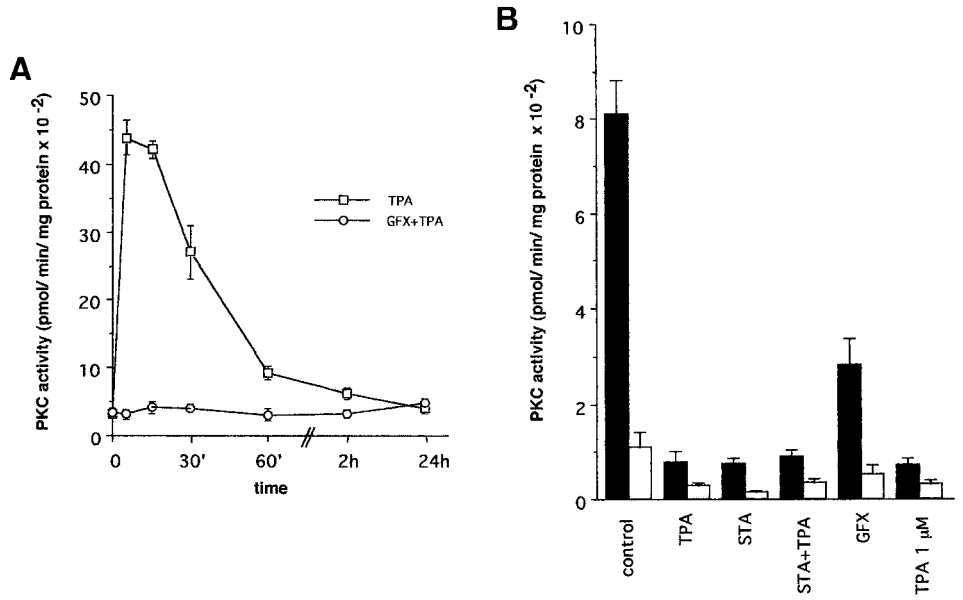


*Fig. 8. A,* activation of PKC by TPA in K562 cells. Cells were treated in serum-free media with 10 nM TPA (□) or pretreated for 1 h with 2 μM GFX prior to TPA addition to 10 nM (*GFX+TPA*; ○). Cells were harvested at different times, and PKC was determined as indicated in "Materials and Methods." *B,* PKC activity in K562 cells after 24 h of treatment with 10 nM TPA, 100 nM STA, 100 nM STA plus 10 nM TPA, and 2 μM GFX. As negative control, the cells were treated for 16 h with 1 μM TPA to achieve complete depletion of PKC. □, measurements obtained in the presence of the PKC pseudosubstrate inhibitor. *Bars,* SD.

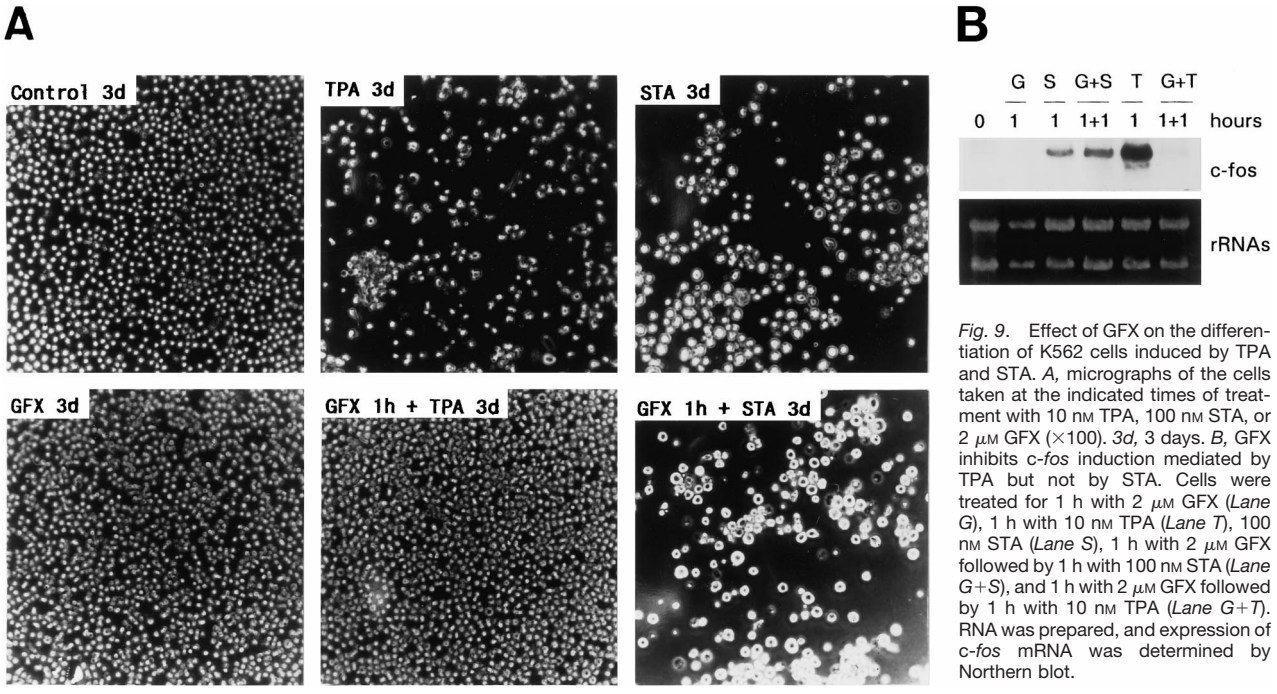


*Fig. 9.* Effect of GFX on the differentiation of K562 cells induced by TPA and STA. *A,* micrographs of the cells taken at the indicated times of treatment with 10 nM TPA, 100 nM STA, or 2 μM GFX (×100). *3d,* 3 days. *B,* GFX inhibits c-*fos* induction mediated by TPA but not by STA. Cells were treated for 1 h with 2 μM GFX (*Lane G*), 1 h with 10 nM TPA (*Lane T*), 100 nM STA (*Lane S*), 1 h with 2 μM GFX followed by 1 h with 100 nM STA (*Lane G+S*), and 1 h with 2 μM GFX followed by 1 h with 10 nM TPA (*Lane G+T*). RNA was prepared, and expression of c-*fos* mRNA was determined by Northern blot.

consequence but does not play a determinant role in the megakaryocytic and monocytic differentiation response of K562 cells.

c-Myc requires dimerization with Max to be active (see "Introduction"). Thus, we next tested whether the ectopic overexpression of Max modifies STA- and TPA-mediated differentiation. We used two K562 sublines in which the expression of *max* is zinc inducible, Kmax12 and Kmax16 (35). After addition of 75 μM $ZnSO_4$ and TPA (10 nM) or STA (100 nM), we analyzed the differentiation by cell morphology, adherence, and NBT reduction. In the presence of zinc, expression of Max was induced, but there were no significant differences in the extent of STA-mediated megakaryocytic differentiation or TPA-mediated monocytic differentiation with respect to untreated cells (not shown).

It was formally possible that the availability of Max protein was limiting in situations where c-Myc is induced. To explore this possibility, we generated double transfectants in which the expression of c-*myc* and *max* are both induced by zinc. To do so, we transfected a K562 subline in which expression of c-Myc is zinc inducible (KmycB; Ref. 15) with a construct carrying a zinc-inducible human *max*

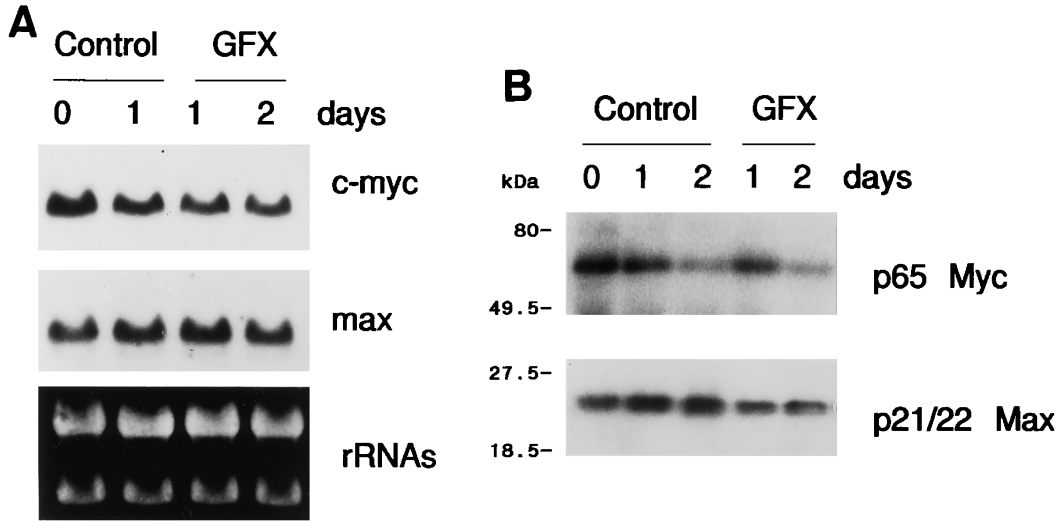


*Fig. 10.* *myc* and *max* expression is not modified in K562 cells treated with GFX. *A,* Northern analysis of RNAs isolated from cells treated with 2 μM GFX for 1 and 2 days. *Control lanes,* cells without drug addition. The same filter was consecutively hybridized to the c-*myc* and *max* probes. A picture of the filter after transfer is shown to assess the loading and integrity of the RNAs. *B,* immunoblot of proteins from cells treated with GFX. Cells were untreated (*control lanes*) or treated with 2 μM GFX for the indicated periods of time. The blots were incubated with anti-Myc and anti-Max antibodies as indicated. *Left,* position of molecular mass markers.

gene (pHEBo-MTmax; Ref. 35). Two transfectant cell lines with zinc-inducible expression of c-*myc* and *max* mRNA, termed Kmyma3 and Kmyma20, were selected (Fig. 12*A*), and the overexpression of Max and c-Myc proteins upon addition of $ZnSO_4$ was verified by immunoblot (Fig. 12*B*). Also, the expression of ectopic c-*myc* and *max* was induced by 75 μM $ZnSO_4$ in cells treated with 10 nM TPA or 100 nM STA, under which conditions endogenous c-*myc* is repressed (Fig. 12*A*). We then tested the differentiation response of Kmyma3 and Kmyma20 after treatment with TPA or STA and found that the differentiation of both cell lines was alike in the presence and absence of zinc. This was assessed by cell morphology, and up-regulation of vimentin and repression of ε-globin (Fig. 12*A*), NBT cytochemical reaction (not shown), and cluster formation (Fig. 12*C*). Similarly, enforced coexpression of c-Myc and Max did not impair the differentiation achieved with lower drug concentrations (2 nM TPA and 50 nM STA). We also generated a double transfectant in which Max expression was zinc inducible, and high levels of constitutive c-*myc* expression were achieved by retroviral infection (LmycSN vector). These cells showed a similar differentiation response, regardless of the induction of *max (*not shown). Altogether, these results indicate that overexpression of c-Myc did not modify monocytic or megakaryocytic differentiation of K562.

## Discussion

The present work has established: (*a*) a new model of *in vitro* megakaryocytic differentiation, *i.e.,* K562 cells treated with the PKC inhibitor staurosporine; (*b*) we show that, although Max expression does not change, c-*myc* gene is down-regulated during monocytic-macrophagic and megakaryocytic differentiation of K562 in a PKC-independent manner; (*c*) we show that PKC activity does not correlate with c-*myc* expression levels in K562; and (*d*) we demonstrate that enforced expression of c-Myc and Max does not inhibit the monocytic-macrophagic and megakaryocytic differentiation induced by TPA or STA.

The differentiation phenotype induced by TPA in K562 cells is usually referred to as "megakaryocytic," based on the expression of markers such as CD41 (glycoprotein IIb), CD61 (glycoprotein IIIa), and platelet-derived growth factor (33, 36). However, in contrast to a widely accepted view, the majority of TPA-treated K562 cells resemble monocytes-macrophages on the basis of cell morphology and ultrastructure, albeit megakaryocyte-like cells are also present. We have also found that treatment of K562 cells with STA induced in most cells a differentiated phenotype that strongly resembled megakaryocytes. Previous reports have shown that STA induced polyploidy in K562 cells (48), but the differentiation phenotype was reported to be the same as that induced by TPA. This could be explained by the fraction of megakaryocyte-like cells, which also appear after TPA treatment, that may be partially responsible for the similar pattern of surface marker expression detected in STA- and TPA-differentiated cells. However, we found that STA-treated cells show highly lobulated nuclei, undergo active endoreduplication, and display demarcation membranes in cytoplasm. All these traits are hallmarks of megakaryocytes. Furthermore, platelet-like forms can be observed in the cytoplasm and conditioned media of STA-treated cells. Other differences between TPA- and STA-induced differentiation include the pattern of distribution of vimentin filaments and the ANAE reaction

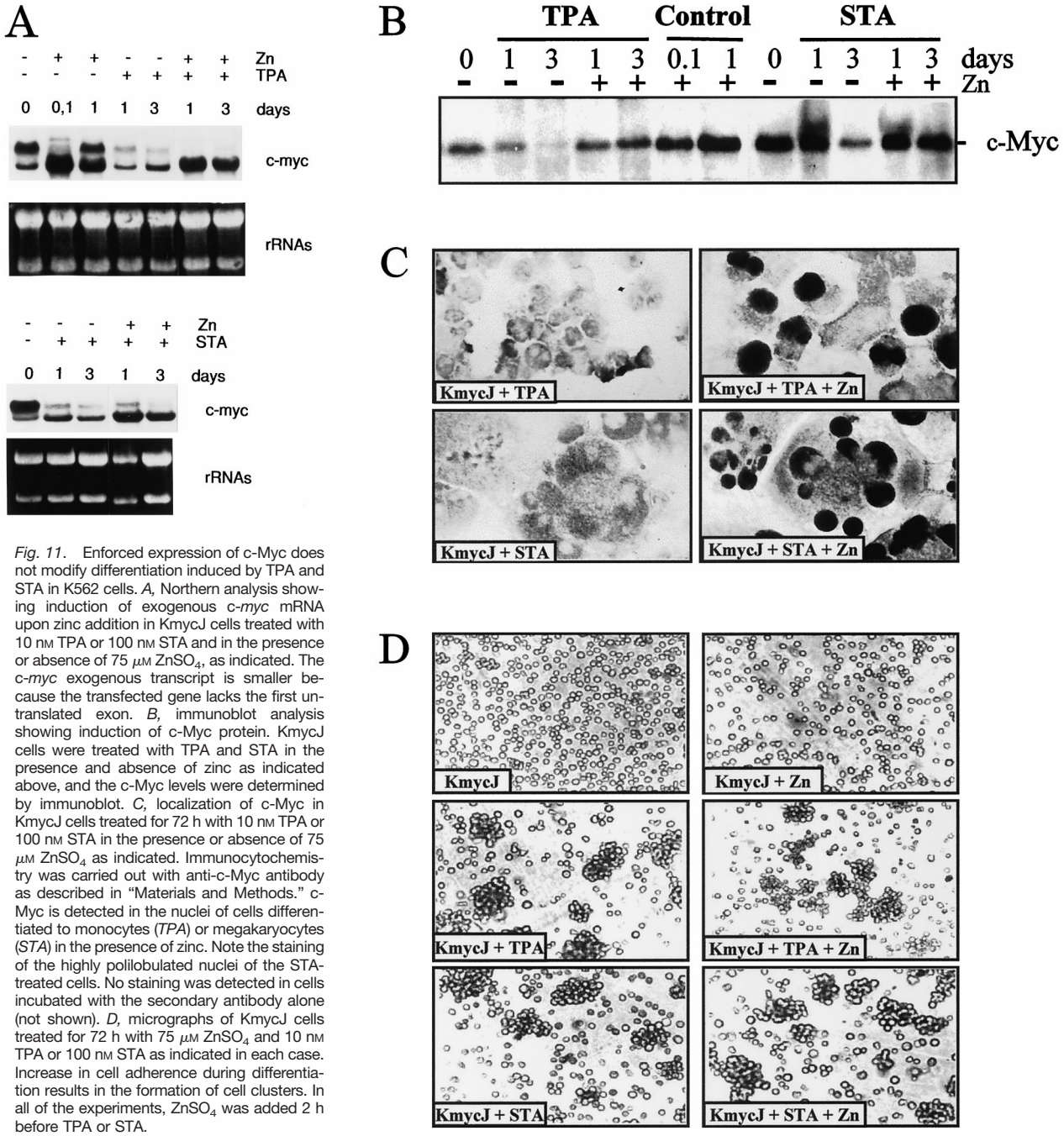


*Fig. 11*. Enforced expression of c-Myc does not modify differentiation induced by TPA and STA in K562 cells. *A,* Northern analysis showing induction of exogenous c-*myc* mRNA upon zinc addition in KmycJ cells treated with 10 nM TPA or 100 nM STA and in the presence or absence of 75 $\mu$M $ZnSO_4$, as indicated. The c-*myc* exogenous transcript is smaller because the transfected gene lacks the first untranslated exon. *B,* immunoblot analysis showing induction of c-Myc protein. KmycJ cells were treated with TPA and STA in the presence and absence of zinc as indicated above, and the c-Myc levels were determined by immunoblot. *C,* localization of c-Myc in KmycJ cells treated for 72 h with 10 nM TPA or 100 nM STA in the presence or absence of 75 $\mu$M $ZnSO_4$ as indicated. Immunocytochemistry was carried out with anti-c-Myc antibody as described in "Materials and Methods." c-Myc is detected in the nuclei of cells differentiated to monocytes (*TPA*) or megakaryocytes (*STA*) in the presence of zinc. Note the staining of the highly polilobulated nuclei of the STA-treated cells. No staining was detected in cells incubated with the secondary antibody alone (not shown). *D,* micrographs of KmycJ cells treated for 72 h with 75 $\mu$M $ZnSO_4$ and 10 nM TPA or 100 nM STA as indicated in each case. Increase in cell adherence during differentiation results in the formation of cell clusters. In all of the experiments, $ZnSO_4$ was added 2 h before TPA or STA.

(negative for STA-treated cells but positive for monocytic TPA-differentiated cells). Finally, there are profound differences in the differentiation kinetics induced by both drugs, *i.e.,* cells require longer exposure to STA than to TPA to become committed. Therefore, K562 cells are a unique model that can be directed into at least three distinct types of differentiation (erythroid, megakaryocytic, and monocytic-macrophagic). Moreover, the megakaryocytic differentiation elicited by STA is not exclusive for the K562 cell line, because STA also mediates megakaryocytic differentiation in KU812 cells, another chronic myeloid leukemia cell line.[4]

Interestingly, the drugs used to induce monocytic or megakaryocytic differentiation were an activator (TPA) and an inhibitor (STA) of PKC. We took advantage of this model to study the relationship between PKC and c-*myc* regula-

[4] N. Ajenjo and J. León, unpublished observations.

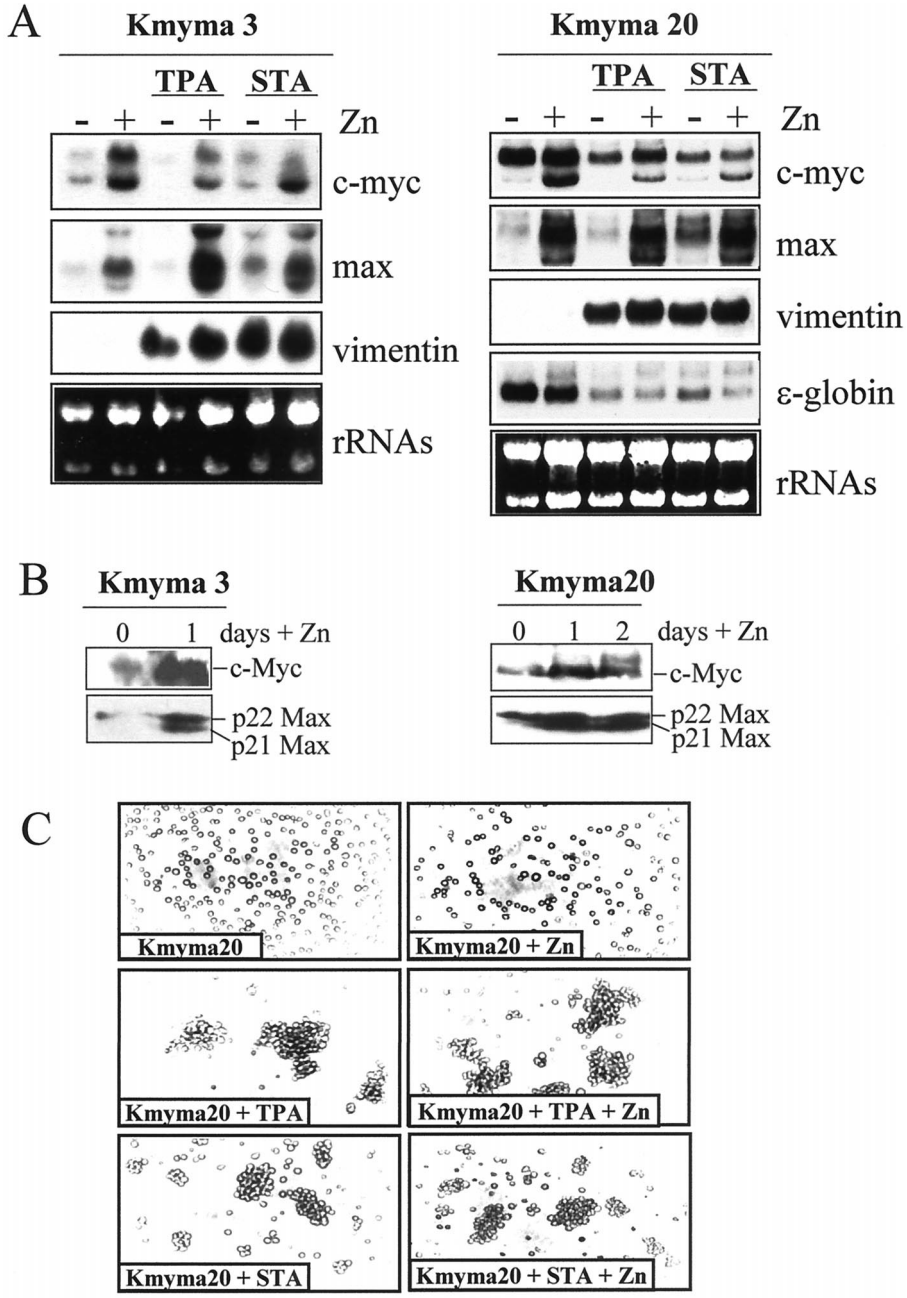


*Fig. 12*. Enforced coexpression of c-Myc and Max does not modify the differentiation induced by TPA and STA in K562 cells. *A,* Northern analysis of c-*myc*, *max*, vimentin, and ϵ-globin of Kmyma3 and Kmyma20 cells treated with 10 nM TPA and 100 nM STA in the absence and presence of 75 $\mu$M $ZnSO_4$ as indicated. *B,* c-Myc and Max induction after zinc addition in Kmyma3 and Kmyma20 cells. Cells were treated with 75 $\mu$M $ZnSO_4$ for 1 and 2 days and the levels of c-Myc and Max were determined by immunoblot. The same filter was used consecutively for c-Myc and Max detection. Only the p21 form of Max was induced after zinc addition because this is the form encoded by the transfected gene. *C,* micrographs of Kmyma20 cells treated for 72 h with 75 $\mu$M $ZnSO_4$, 10 nM TPA, and 100 nM STA, as indicated in each case. Increase in cell adherence during differentiation results in the formation of cell clusters. In all of the experiments, $ZnSO_4$ was added 2 h before TPA or STA.

tion, as well as the effect of c-*myc* overexpression on both differentiation pathways. Similarly to many differentiation models, c-*myc* expression is down-regulated during monocytic macrophagic and megakaryocytic differentiation. Conversely, *max* expression is kept constant in both processes. These results suggest that the levels of transcriptionally active Myc-Max complexes are low in K562 cells differentiated into monocyte-macrophages or megakaryocytes, and that the majority of the Max proteins would be either in Max-Max homodimers or complexed with proteins of the Mad family (Mad1, Mxi1, Mad3, and Mad4), as demonstrated in other differentiation models (13, 14, 49, 50).

In all myeloid cell lines thus far investigated, the expression of c-*myc* is suppressed upon differentiation induced by TPA (9–12). The results of the present work extend this finding to STA-mediated differentiation. The issue of whether the suppression of c-Myc levels correlate with differentiation or with PKC activity has been subjected to controversy, mostly based on studies performed in HL60 cell lines (22–24). To tackle this problem, we measured PKC activities in TPA- and STA- treated K562 cells. As expected, STA inhibited PKC activity and TPA activated PKC after short treatment times. However, PKC activity was also low after 24 h of treatment with TPA, when the cells are irreversibly growth arrested and

differentiated. It is known that chronic exposure to TPA results in PKC down-regulation, although in other cell types as murine fibroblasts (51) and chicken E26-infected myeloblasts (19), this effect requires much higher TPA concentrations than in K562. Thus, our results opened the possibility that the repression of c-*myc* expression is a consequence of the PKC down-regulation, in agreement with previous reports in HL60 cells (24, 25). However, the inhibition of PKC by the specific inhibitor GFX did not provoke any effect on growth and differentiation and did not down-regulate c-*myc*, whereas it completely blocked TPA-mediated differentiation. Altogether, our results indicate that: (*a*) the expression of c-*myc* and *max* in K562 are unrelated to PKC activity but are linked to the differentiation process; and (*b*) TPA induces differentiation of K562 by a PKC-dependent mechanism. Also, it must be noted that STA also inhibits other protein kinases such as protein kinase A (41) and cyclin-dependent kinase 2 (42); therefore, STA-mediated differentiation might involve mechanisms other than PKC inhibition.

Constitutive overexpression of c-Myc inhibits differentiation in most hematopoietic cell models analyzed, including murine erythroid (52–54) and monocytic (55, 56) cell lines. Supression of c-*myc* expression with antisense mRNA or oligonucleotides (26–28) results in spontaneous differentiation of human HL60 cells, although these findings have not been confirmed in other studies (57–60). We found that c-Myc does not play a role in K562 commitment to myeloid differentiation, at least at the expression levels achieved in the transfected cells. Although significant amounts of c-Myc are present in the nuclei of transfected cells, differentiated with TPA or STA, a possible explanation for the lack of effect of c-Myc is that the total expression levels of c-Myc obtained in our transfectants are not sufficient to achieve a differentiation block. Although this possibility cannot be formally excluded, ectopic c-Myc provokes down-regulation of endogenous c-*myc* mRNA expression. Moreover, in the same cell lines, similar c-Myc levels impair erythroid differentiation (15). Also, it could be possible that Max concentration is a limiting factor for c-Myc functions in this model. We ruled out this possibility because double transfectants with concomitant induction of Max and c-Myc are efficiently differentiated by TPA and STA. Likewise, we found that Max overexpression alone had no apparent effect on the differentiation induced by STA and TPA.

There are several examples where enforced expression of c-*myc* or v-*myc* do not inhibit terminal differentiation, such as murine keratinocytes (57, 58), murine muscle cells (59, 60), rat oligodendrocyte progenitors (61) and quail chondroblasts (62), and mouse F9 teratocarcinoma cells (63). The present study with K562 cells is the first report on a similar finding in cells of myeloid lineage. Our results are in contrast with the described inhibition by v-*myc* of TPA-mediated differentiation of U937 (64). We do not know the reason for this difference, but it may reside in the different origin of these cell lines (K562 derives from a chronic myeloid leukemia, whereas U937 derives from a malignant histiocytosis) and the transfected gene (v-*myc* in U937 and c-*myc* in K562). Conversely to the monopotent U937 cells, K562 can be differentiated toward erythroid, monocytic, and megakaryocytic lineages. The fact that monocytic and megakaryocytic differentiation are unaffected by c-Myc overexpression is in striking contrast with the partial inhibition of erythroid differentiation by ectopic overexpression of c-*myc* (15). Thus, the K562 model demonstrates diverging roles of the c-Myc/Max complex in the control of the commitment to distinct differentiation lineages in human myeloid cells.

## Materials and Methods

**Cell Culture and Transfections.** K562 cell line was obtained from American Type Culture Collection. Cells were grown in RPMI 1640 medium (Life Technologies, Inc., Gaithersburg, MD) supplemented with 8% FCS (Biochrome, Berlin, Germany) and gentamicin (80 $\mu$g/ml). KmycB and KmycJ are cell lines described previously with inducible expression of c-*myc* (15). Kmax12 is a cell line with inducible expression of *max* described previously (35). KmycB ($2 \times 10^6$ cells) were electroporated (260 V and 1 mF; Bio-Rad Gene Pulser apparatus) with 20 $\mu$g of pHEBoMT-max (35) and 5 $\mu$g of LXSN, a plasmid encoding G418 resistance (65). After electroporation, cells were incubated for 48 h, and 0.5 mg/ml of G418 was added. Transfectant cell clones were selected by limiting dilution. Cell densities were kept below $10^6$/ml. When indicated, exponentially growing cells at a concentration of $2.5 \times 10^5$ cells/ml were treated with TPA (Sigma, St. Louis, MO), STA (Roche Molecular Biochemicals, Barcelona, Spain), or GFX (Calbiochem, Cambridge, MA). Cell growth and viability were assayed by hemocytometer and the trypan blue exclusion test.

**Differentiation Marker Determinations.** Morphological differentiation was monitored by examining cell preparations stained with May-Grünwald Giemsa and assessed using established cytological criteria. The fraction of hemoglobin-producing cells was scored by benzidine staining as described previously (29). NBT dye reduction was used to monitor monocyte/granulocytic differentiation (66). The presence of ANAE (nonspecific esterase) was determined by cytochemistry with a commercial kit (Sigma). The expression of cell surface markers was measured by quantitative fluorescence analysis using an Epics Profile II flow cytometer (Coulter Electronics). The cells were incubated for 45 min at 4°C with the appropriate monoclonal antibodies. At least 10,000 cells were analyzed for each antibody for light scattering and fluorescence intensity. The antibodies used were: anti-glycoprotein IIIa (CD61) and CD14 (FITC-conjugated; Dako, Copenhagen, Denmark). Nonspecific fluorescence was determined by using isotypic negative control antibodies.

**DNA Analysis by Flow Cytometry.** To determine DNA content, cells were collected by centrifugation, washed once in PBS, and resuspended in citrate buffer (50 mM sodium citrate, 0.1 mg/ml RNase A, and 10 $\mu$g/ml propidium iodide). After incubation at 37°C for 30 min, the stained cells were analyzed in a FACScan flow cytometer (Becton Dickinson) using the CellQuest software. To analyze the fraction of cells undergoing DNA synthesis (S phase), cells were cultured in the presence of 20 $\mu$M BrdUrd for 12 h. After fixation in 70% ethanol at 4°C for 15 min, the cells were washed and resuspended in PBS. The genomic DNA was denaturated by incubation of fixed cells in 1 N HCl-0.5% Tween 20 at 37°C for 15 min. After centrifugation, cells were washed twice in PBS-2% FCS and incubated with 50 $\mu$l of anti-BrdUrd monoclonal antibody (Amersham) diluted in PBS-0.1% Triton X-100 for 20 min on ice. After washing in PBS-2% FCS, cells were analyzed by flow cytometry in the presence of propidium iodide as above.

**Electron Microscopy.** Cell pellets were fixed in freshly prepared 3% glutaraldehyde in PBS for 60 min, dehydrated in acetones, and embedded in araldite. Ultrathin sections were stained with uranyl acetate and lead citrate and examined and photographed with a Phillips EM 208 electron microscope.

**Immunocytochemistry.** Cytospin preparations were fixed in freshly prepared 3.7% paraformaldehyde in PBS (pH 7.4) at room temperature for 15 min with gentle agitation. For immunofluorescence, the cells were made permeable in 0.2% Triton X-100 at room temperature for 5 min and natural paraformaldehyde fluorescence was blocked with 0.1 M glycine in PBS. After three washes in PBS-0.1%

Tween 20 (PBS-T; 2–3 min each), the cells were incubated for 1 h at room temperature with a monoclonal anti-vimentin antibody (V9; Roche Molecular Molecular Biochemicals) diluted 1:10. The slides were rinsed in PBS-T for 5 min and incubated for 45 min at room temperature with an anti-mouse FITC-conjugated secondary (Vector, Burlingame, CA) diluted 1:100. After washing with PBS, the samples were mounted with Vectashield (Vector) and examined with a confocal laser microscope (Bio-Rad 1024) using argon ion (488 nm) to excite FITC. For c-Myc detection, cells were fixed with paraformaldehyde as above, treated with 3% $H_2O_2$ in cold methanol, washed with PBS-T, and incubated for 1 h with a monoclonal anti-c-Myc antibody (C-33, diluted 1:10; Santa Cruz Biotechnology, Santa Cruz, CA). The slides were washed in PBS-T and incubated with biotinylated anti-mouse IgG and ExtrAvidin peroxidase (Sigma) and revealed using 3,3′-diaminobenzidine as the peroxidase substrate.

**RNA Analysis.** Total RNA was isolated from cells by the acid guanidine thiocyanate method (67). RNA samples (15 $\mu$g/lane) were electrophoresed on 1% agarose-formaldehyde gels and transferred to nitrocellulose membranes (Millipore, Bedford, MA) as described (68), except that 1 $\mu$g of ethidium bromide was added to each RNA sample prior to gel loading. A picture of the filter under UV light was obtained after transfer to assess the amount and integrity of the rRNAs. The Northern blots were hybridized at 42°C in 40% formamide, 5% dextran sulfate, 0.8 M NaCl, 50 mM sodium phosphate (pH 7), 0.2% SDS, 150 $\mu$g of denatured salmon sperm DNA/ml, and DNA probe labeled with [$^{32}$P]dCTP by random primed labeling (Pharmacia kit). The filters were washed to a final stringency of 0.5× SSC (0.15 M NaCl, 0.15 M sodium citrate) and 0.1% SDS at 65°C and autoradiographed at −70°C. The signals were quantified with a Bio-Rad Molecular Imager GS-250 apparatus. Probes for human c-*myc*, *max*, $\epsilon$-globin, and vimentin were as described (15). Probe for human c-*fos* probe was the 1.5-kb *Pst*I fragment from pFOS-1 (obtained from American Type Culture Collection).

**Immunoblots.** For c-Myc and Max determinations, cell pellets were lysed in a solution containing 100 mM Tris (pH 6.8), 8% $\beta$-mercaptoethanol, 4% SDS, and 20% glycerol. The lysates were boiled for 5 min and passed through 21-gauge needle to shear the DNA. Protein content was measured using Bio-Rad Protein Assay. Forty $\mu$g of protein/lane were separated in 10% acrylamide gels and transferred to polyvinylidene difluoride membranes (Millipore), using a semidry electroblotter (Millipore) and a buffer containing 10 mM Trizma, 96 mM glycine, and 10% methanol. c-Myc protein was detected by the anti-Myc antibody (1–9E10; Santa Cruz Biotechnology). Max was detected with a rabbit polyclonal antibody (Upstate Biotechnology, Lake Placid, NY). Proteins were detected by chemiluminescent (ECL; Amersham, Buckinghamshire, United Kingdom).

**PKC Activity Determinations.** Cells incubated in the presence of TPA or STA were harvested in a buffer containing 20 mM Tris (pH 7.5), 0.5 mM EDTA, 0.5 mM EGTA, 0.5% Triton X-100, 25 $\mu$g/ml leupeptin, 25 $\mu$g/ml aprotinin, and 10 mM $\beta$-mercaptoethanol. Cells were disrupted by passage through a 26-gauge needle and centrifuged for 15 min at 4 C at 12,000 × *g*. Protein concentration in the supernatants was determined by the Bio-Rad kit. PKC activity was determined using a kit (Life Technologies, Inc.) essentially as described by the manufacturers without adding TPA or phosphatidylserine-containing liposomes. PKC activity in cell extracts was determined by measuring phosphotransferase activity to a synthetic peptide derived from myelin basic protein (69). The reaction was carried out with 4 $\mu$Ci/ml [$\gamma$-$^{32}$P]ATP, 20 $\mu$M ATP, 20 mM $MgCl_2$, and 1 mM CaCl in the presence or absence of 20 $\mu$M pseudosubstrate peptide PKC (19–36), a potent inhibitor of PKC (maximal activity on $\alpha$, $\beta$, and $\gamma$ isoforms) used as a control for PKC specificity of the assay (70).

## Acknowledgments

We are grateful to Pilar Frade and Carolina Añibarro for excellent technical assistance; M. Angeles Cuadrado for help with flow cytometry; M. Angeles Ros for image analysis; Fernando de la Cruz for reagents; Riccardo Dalla Favera, Martin Eilers, and Robert Eisenman for plasmids; and Miguel Lafarga, Steven Collins, and David Aaronson for critical reading of the manuscript.

## References

1. Marcu, K. B., Bossone, S. A., and Pattel, A. J. MYC function and regulation. Annu. Rev. Biochem., *61:* 809–860, 1992.

2. Henriksson, M., and Lüscher, B. Proteins of the Myc network: essential regulators of cell growth and differentiation. Adv. Cancer Res., *68:* 109–182, 1996.

3. Amati, B., Alevizopoulos, K., and Vlach, J. Myc and the cell cycle. Front. Biosci., *3:* d250–d268, 1998.

4. Bouchard, C., Staller, P., and M. Eilers. Control of cell proliferation by Myc. Trends Cell Biol., *8:* 202–206, 1998.

5. Blackwood, E. M., and Eisenman, R. N. Max: a helix-loop-helix zipper protein that forms a sequence-specific DNA-binding complex with Myc. Science (Washington DC), *251:* 1211–1217, 1991.

6. Prendergast, G. C., Lawe, D., and Ziff, E. B. Association of Myn, the murine homologue of Max, with c-Myc stimulates methylation-sensitive DNA binding and Ras cotransformation. Cell, *65:* 395–407, 1991.

7. Grandori, C., and Eisenman, R. N. Myc target genes. Trends Biochem. Sci., *22:* 177–181, 1997.

8. Dang, C. V. c-Myc target genes involved in cell growth, apoptosis and metabolism. Mol. Cell. Biol., *19:* 1–11, 1999.

9. Einat, M., Resnitzky, D., and Kimchi, A. A close link between reduction of c-*myc* expression by interferon and G0/G1 arrest. Nature (Lond.), *313:* 597–600, 1985.

10. Grosso, L. E., and Pitot, H. C. Transcriptional regulation of c-myc during chemically induced differentiation of HL-60 cultures. Cancer Res., *45:* 847–850, 1985.

11. Long, M. W., Heffner, C. H., Williams, J. L., and Prochownik, E. V. Regulation of megakaryocyte phenotype in human erythroleukemia. J. Clin. Invest., *85:* 1072–1084, 1990.

12. Derigs, H. G., Morgan, D. A., Hoffman, R., Litz, S. L., Srour, E. F., Brandt, J. E., and Boswell, H. S. AP-1/c-jun and c-myc regulation during megakaryocytic differentiation of a human bipotential growth factor-dependent cell line. Platelets, *6:* 24–30, 1995.

13. Ayer, D. E., and Eisenman, R. N. A switch from Myc:Max to Mad:Max heterocomplexes accompanies monocyte/macrophage differentiation. Genes Dev., *7:* 2110–21119, 1993.

14. Larsson, L-G., Pettersson, M., Öberg, F., Nilsson, K., and Lüscher, B. Expression of *mad, mxi1*, *max* and c-*myc* during induced differentiation of hematopoietic cells: opposite regulation of *mad* and c-*myc*. Oncogene, *9:* 1247–1252, 1994.

15. Delgado, M. D., Lerga, A., Cañelles, M., Gómez-Casares, M. T., and León, J. Differential regulation of Max and role of c-Myc during erythroid and myelomonocytic differentiation of K562 cells. Oncogene, *10:* 1659–1665, 1995.

16. Nishikawa, M., and Shirakawa, S. The expression and possible roles of protein kinase C in haemopoietic cells. Leuk. Lymphoma, *8:* 201–211, 1992.

17. Aihara, H., Asaoka, Y., Yoshida, K., and Nishizuka, Y. Sustained activation of protein kinase C is essential to HL-60 cell differentiation to macrophage. Proc. Natl. Acad. Sci. USA, *88:* 11062–11067, 1991.

18. Tonetti, D. A., Henning-Chubb, C., Yamanishi, D., and Huberman, E. Protein kinase C-$\beta$ is required for macrophage differentiation of human HL-60 leukemia cells. J. Biol. Chem., *269:* 23230–23235, 1994.

19. Rossi, F., McNagny, K. M., Smith, G., Frampton, J., and Graf, T. Lineage commitment of transformed haematopoietic progenitors is determined by the level of PKC activity. EMBO J., *15:* 1894–1901, 1996.

20. Ebeling, J. G., Vandenbark, G. R., Kuhn, L. J., Ganong, B. R., Bell, R. M., and Niedel, J. E. Diacylglycerols mimic phorbol diester induction of leukemic cell differentiation. Proc. Natl. Acad. Sci. USA, *82:* 815–819, 1985.

21. Murray, N. R., Baumgardner G. P., Burns D. J., and Fields, A. P. Protein kinase C isotypes in human erythroloukemia (K562) cell proliferation and differentiation. J. Biol. Chem., *268:* 15847–15853, 1993.

22. Hong, Y., Martin, J. F., Vainchenker, W., and Erusallimsky, J. D. Inhibition of protein kinase C suppresses megakaryocytic differentiation

and stimulates erythroid differentiation in HEL cells. Blood, *87:* 123–131, 1996.

23. Gailani, D., Cadwell, F. J., O'Donnell, P. S., Hromas, R. A., and Macfarlane, D. E. Absence of phorbol ester-induced down-regulation of *myc* protein in the phorbol ester-tolerant mutant of HL-60 promyelocytes. Cancer Res., *49:* 5329–5333, 1989.

24. Simpson, R. U., Hsu, T., Wendt, M. D., and Taylor, J. M. 1,25-Dihydroxyvitamin D3 regulation of c-*myc* protooncogene transcription. Possible involvement of protein kinase C. J. Biol. Chem., *264:* 19710–19715, 1989.

25. Berstein, S. H., Kharbanda, S. M., Sherman, M. L., Stone, R. M., and Kufe, D. W. Inhibition of protein kinase C is associated with a decrease in c-*myc* expression in human myeloid leukemia cells. FEBS Lett., *294:* 73–76, 1991.

26. Holt, J. T., Redner, R. L., and Nienhuis, A. W. An oligomer complementary to c-*myc* mRNA inhibits proliferation of HL-60 promyelocytic cells and induces differentiation. Mol. Cell. Biol., *8:* 963–973, 1988.

27. Bacon, T. A, and Wickstrom, E. Daily addition of an anti-c-myc DNA oligomer induces granulocytic differentiation of human promyelocytic leukemia HL-60 cells in both serum-containing and serum-free media. Oncogene Res., *6:* 21–32, 1991.

28. Yokoyama, K., and Imamoto, F. Transcriptional control of the endogenous MYC protooncogene by antisense RNA. Proc. Natl. Acad. Sci. USA, *84:* 7363–7367, 1987.

29. Rowley, P. T., Ohlsson-Wilhelm, B. M., Farley, B. A., and LaBella, S. Inducers of erythroid differentiation in K562 human leukemia cells. Exp. Hematology, *9:* 32–37, 1981.

30. DeLuca, L. C., Mitchell, T., Spriggs, D., and Kufe, D. W. Induction of terminal differentiation in human K-562 erythroleukemia cells by arabinofuranosyl cytosine. J. Clin. Investig., *74:* 821–827, 1984.

31. Sutherland, J. A., Turner, A. R., Mannoni, P., McGann, L. E., and Turc, J. M. Differentiation of K562 leukemia cells along erythroid, macrophage, and megakaryocyte lineages. J. Biol. Response Modif., *5:* 250–262, 1986.

32. Leary, J. F., Ohlsson-Wilhelm, B. M., Giuliano, R., LaBella, S., Farley, B., and Rowley, P. T. Mutipotent human hematopoietic cell line K562: lineage-specific constitutive and inducible antigens. Leuk. Res., *11:* 807–815, 1987.

33. Alitalo, R. Induced differentiation of K562 leukemia cells: a model for studies of gene expression in early megakaryoblasts. Leuk. Res., *14:* 501–514, 1990.

34. Delgado, M. D., Quincoces, A. F., Gómez-Casares, M. T., Cuadrado, M. A., Richard, C., and León, J. Differential expression of *ras* protooncogenes during induced differentiation of human erythroleukemia cells. Cancer Res., *52:* 5979–5984, 1992.

35. Cañelles, M., Delgado, M. D., Hyland, K. M., Lerga, A., Richard, C., Dang, C. V., and León, J. Max and inhibitory c-Myc mutants induce erythroid differentiation and resistant to apoptosis in human leukemia cells. Oncogene, *14:* 1315–1327, 1997.

36. Tani, T., Ylänne, J., and Virtanen, I. Expression of megakaryocytic and erythroid properties in human leukemic cells. Exp. Hematol., *24:* 158–168, 1996.

37. Vanags, D. M., Orrenius, S., and Aguilar-Santelises, M. Alterations in the Bcl-2/Bax protein levels in platelets form part of an ionomycin-induced process. Br. J. Haematol., *99:* 824–831, 1997.

38. Zauli, G., Vitale, M., Falcieri, E., Gibellini, D., Bassini, A., Celeghini, C., Columbaro, M., and Capitani, S. *In vitro* senescence and apoptotic cell death of human megakaryocytes. Blood, *90:* 2234–2243, 1997.

39. Isenberg, W. M., and Bainton, D. F. Megakaryocyte and platelet structure. *In:* R. Hoffman, E. J. Benz, S. J. Shattil, B. Furie, H. J. Cohen, and L. E. Silberstein (eds.), Hematology. Basic Principles and Practice, Ed. 2, pp. 1516–1524. NY: Churchill Livinstone, 1995.

40. Gómez-Casares, M. T., Delgado, M. D., Lerga, A., Crespo, P., Quincoces, A. F., Richard, C., and León, J. Down-regulation of C-*MYC* gene is not obligatory for growth inhibition and differentiation of human myeloid leukemia cells. Leukemia (Baltimore), *7:* 1824–1833, 1993.

41. Goodnight, J., Mishak, H., and Mushinski, J. F. Selective involvement of protein kinase C isozymes in differentiation and neoplastic transformation. Adv. Cancer Res., *64:* 159–209, 1994.

42. Walker, D. H. Small-molecule inhibitors of cyclin-dependent kinases: molecular tools and potential therapeutics. Curr. Top. Microbiol. Immunol., *227:* 149–165, 1998.

43. Hocevar, B. A., Morrow, D. M., Tykocinski, M. L., and Fields, A. P. Protein kinase C isotypes in human erythroleukemia cell proliferation and differentiation. J. Cell Sci., *101:* 671–679, 1992.

44. Toullec, D., Pianetti, P., Coste, H., Bellevergue, P., Grand-Perret, T., Ajakane, M., Baudet, V., Boissin, P., Boursier, E., Loriolle, F., Duhamel, L., Charon, D., and Kirilowsky, J. The bisindolylmaleimide GF 109203X is a potent and selective inhibitor of protein kinase C. J. Biol. Chem., *266:* 15771–15781, 1991.

45. Alitalo, R., Partanen, J., Pertovaara, L., Holtta, E., Sistonen, L., Andersson, L., and Alitalo, K. Increased erythroid potentiating activity/tissue inhibitor of metalloproteinases and jun/*fos* transcription factor complex characterize tumor promoter-induced megakaryoblastic differentiation of K562 leukemia cells. Blood, *75:* 1974–1982, 1990.

46. Grignani, F., Lombardi, L., Inghirami, G., Sterna, S. L., Cechova, K., and Dalla-Favera, R. Negative autoregulation of c-*myc* gene expression is activated in transformed cells. EMBO J., *9:* 3913–3922, 1990.

47. Facchini, L. M., Chen, S., Marhin, W. W., Lear, J. N., and Penn, L. Z. The Myc negative autoregulation mechanism requires Myc-Max association and involves the c-*myc* P2 minimal promoter. Mol. Cell. Biol., *17:* 100–114, 1997.

48. Yen, A., Varvayanis, S., and Platko, J. D. 12-*O*-Tetradecanoylphorbol-13-acetate and staurosporine induce increased retinoblastoma tumor suppressor gene expression with megakaryocytic differentiation of leukemia cells. Cancer Res., *53:* 3085–3091, 1993.

49. Hurlin, P. J., Foley, K. P., Ayer, D. E., Eisenman, R. N., Hanahan, D., and Arbeit, J. M. Regulation of Myc and Mad during epidermal differentiation and HPV-associated tumorigenesis. Oncogene, *11:* 2487–2501, 1995.

50. Larsson, L. G., Bahram, F., Burkhardt, H., and Luscher, B. Analysis of the DNA-binding activities of Myc/Max/Mad network complexes during induced differentiation of U-937 monoblasts and F9 teratocarcinoma cells. Oncogene, *15:* 737–748, 1997.

51. Rodriguez-Peña, A., and Rozengurt, E. Disappearance of $Ca^{2+}$-sensitive phospholipid-dependent protein kinase activity in phorbol ester-treated 3T3 cells. Biochem. Biophys. Res. Commun., *120:* 1053–1059, 1984.

52. Coppola, J. A., and Cole, M. D. Constitutive c-*myc* oncogene expression blocks mouse erythroleukemia cell differentiation but not commitment. Nature (Lond.), *320:* 760–763, 1986.

53. Dmitrovski, E., Kuehk, W. M., Hollins, G. F., Kirsch, I. R., Bender, T. P., and Segal, S. Expression of a transfected human c-*myc* oncogene inhibits differentiation of a mouse erythroleukemia cell line. Nature (Lond.), *322:* 748–750, 1986.

54. Prochownik, E. V., Kukowska, J., and Rodgers, C. c-*myc* antisense transcripts accelerate differentiation and inhibit $G_1$ progression in murine erythroleukemia cells. Mol. Cell. Biol., *8:* 3683–3695, 1988.

55. Chisholm, O., Stapleton, P., and Symonds, G. Constitutive expression of exogenous myc in myelomonocytic cells: acquisition of a more transformed phenotype and inhibition of differentiation induction. Oncogene, *7:* 1827–1836, 1992.

56. Hoffman-Liebermann, B., and Liebermann, D. A. Interleukin-6- and leukemia inhibitory factor-induced terminal differentiation of myeloid leukemia cells is blocked at an intermediate stage by constitutive c-*myc*. Mol. Cell. Biol., *11:* 2375–2381, 1991.

57. Dotto, G. P., Gilman, M. Z., Maruyama, M., and Weinberg, R. A. c-*myc* and c-*fos* expression in differentiating mouse primary keratinocytes. EMBO J., *11:* 2863–2857, 1986.

58. Gandarillas, A., and Watt, F. c-Myc promotes differentiation of human epidermal stem cells. Genes Dev., *11:* 2869–2882, 1997.

59. Schneider, M. D., Perryman, M. B., Payne, P. A., Spizz, G., Roberts, R., and Olson, E. N. Autonomous expression of c-*myc* in BC3H1 cells partially inhibited but does not prevent myogenic differentiation. Mol. Cell.

Biol., *7:* 1973–1977, 1987.

60. Crescenzi, M., Crouch, D. H., and Tato, F. Transformation by *myc* prevents fusion but not biochemical differentiation of C212 myoblasts: mechanisms of phenotypic correction in mixed culture with normal cells. J. Cell. Biol., *125:* 1137–1145, 1994.

61. Barnett, S. C., and Crouch, D. H. The effect of oncogenes on the growth and differentiation of oligodendrocyte type 2 astrocyte progenitor cells. Cell Growth Differ., *6:* 69–80, 1995.

62. Alema, S., Tato, F., and Boettiger, D. *myc* and *src* oncogenes have complementary effects on cell proliferation and expression of specific extracellular matrix components in definitive chondroblasts. Mol. Cell. Biol., *5:* 538–544, 1985.

63. Nishikura, K., Kim, U., and Murray, J. M. Differentiation of F9 cells is independent of c-*myc* expression. Oncogene, *5:* 981–988, 1990.

64. Larsson, L-G., Ivhed, I., Gidlund, M., Pettersson, U., and Vennström, B. Phorbol ester-induced terminal differentiation is inhibited in human U-937 monoblastic cells expressing a v-*myc* oncogene. Proc. Natl. Acad. Sci. USA, *85:* 2638–2642, 1988.

65. Miller, D., Miller, D. J., Garcia, J. V., and Lynch, C. M. Use of retroviral vectors for gene transfer and expression. Methods Enzymol., *217:* 581–599, 1993.

66. Yam, L., Li, C., and Crosby, W. Cytochemical identification of monocytes and granulocytes. Am. J. Clin. Pathol., *55:* 283–291, 1971.

67. Chomczynski, P., and Sacchi, N. Single step method for RNA isolation by acid guanidinium thiocyanate-phenol-chloroform extraction. Anal. Biochem., *162:* 156–159, 1987.

68. Sambrook, J., Fritsch, E. F., and Maniatis, T. Molecular Cloning: A Laboratory Manual. Cold Spring Harbor, NY: Cold Spring Harbor Laboratory, 1989.

69. Yasuda, I., Kishimoto, A., Tanaka, S., Tominaga, M., Sakurai, A., and Nishizuka, Y. A synthetic peptide substrate for selective assay of protein kinase C. Biochim. Biophys. Res. Commun., *166:* 1220–1227, 1990.

70. House, C., and Kemp, B. E. Protein kinase C contains a pseudosubstrate prototype in its regulatory domain. Science (Washington DC), *238:* 1726–1728, 1987.